

Electronic Supplementary Information

Heteroleptic Chiral Bis(phthalocyaninato) Terbium Double- Decker Single-Ion Magnets

Yuxiang Chen,^a Fang Ma,^b Yuehong Zhang,^a Luyang Zhao,^c Kang Wang,^a Dongdong
Qi,^a Hao-Ling Sun,*^b and Jianzhuang Jiang*^a

Computational details of electrostatic potential

The DFT method of M06-GD3BJ/6-311+G(2df,p)/SDD was used to calculate the electronic structure of **R-1**.^{S1} All the calculations were carried out by using *Gaussian* 09 (version D.01),^{S2} *Multiwfn* (Version 3.4 dev),^{S3} and *VMD* (Version 1.9.1)^{S4} programs.

The electrostatic potential can be calculated using the following equation:

$$V_{ESP}(r) = V_{nuc}(r) + V_{ele}(r) = \sum_A \frac{Z_A}{|r - R_A|} - \int \frac{\rho(r')}{|r - r'|} dr'$$

where V_{ESP} is the total electrostatic potential, V_{nuc} is the electrostatic potential of all the nucleus, V_{ele} is the electrostatic potential of the whole electronic cloud, Z_A is the atomic number of each nucleus, and ρ is the electronic density.

After the geometric optimization, the electronic density can be divided into two parts, including the contributions from terbium atom (named as ρ_{Tb}) and peripheral ligands (named as ρ_L).

$$\rho(r) = \rho_{Tb}(r) + \rho_L(r)$$

$$\rho_{Tb}(r) = \sum_{i \in Tb} \mu_i C_{l,i} \chi_l(r)$$

$$\rho_L(r) = \sum_{i \notin Tb} \mu_i C_{l,i} \chi_l(r)$$

where μ_i is the occupying number of the i th orbital; χ_l is the l th basis function in the i th orbital; $C_{l,i}$ is the element of l th row, and j th column in the expansion coefficient matrix.

When ρ_{Tb} is set to zero, the electrostatic potential of ligands (V_L) can be independently considered in the following manner.

$$V_L(r) = V_{nuc \neq Tb}(r) + V_{ele \neq Tb}(r) = \sum_{A \neq Tb} \frac{Z_A}{|r - R_A|} - \int \frac{\rho_L(r')}{|r - r'|} dr'$$

It is worth noting that the sample dots of *Gaussian*-type cube file are specially set for **R-1** (unit: Bohr, defined in *Gaussian 09 User's Reference*, Manual Version 8.5, Pages 307-309):

449	-4.000604	-3.998980	-4.034339
40	0.205128	0.000000	0.000000
40	0.000000	0.205128	0.000000
40	0.000000	0.000000	0.205128

The above cubes are defined at the *Output File Formats* in the explanation of the *cubegen* keyword. (*Gaussian 09 User's Reference*, Manual Version 8.5, Page 309)

In addition, the electrostatic potential of ligands is drawn on a 2.015 Å radius sphere centered at the Tb³⁺ position caused by the ligands. When the potential projection is drawn in VMD (Version 1.9.1), the detailed setting code is as following:

```
mol new L.cube
mol addfile sphere(cube
mol delrep 0 top
mol representation CPK 0.3 0.3 50.0 50.0
mol addrep top
mol representation Isosurface 0.0001 1 0 0 1 1
mol color Volume 0
mol addrep top
mol scaleminmax top 1 -2.0 1.0
color scale method BGR
color Display Background white
```

where *L.cube* is the cube file of V_L , while *sphere.cube* is an electronic density cube file in which only one hydrogen atom locates at the Tb³⁺ position. The sole usage of *sphere.cube* is the generation of a sphere centered in the Tb³⁺ position.

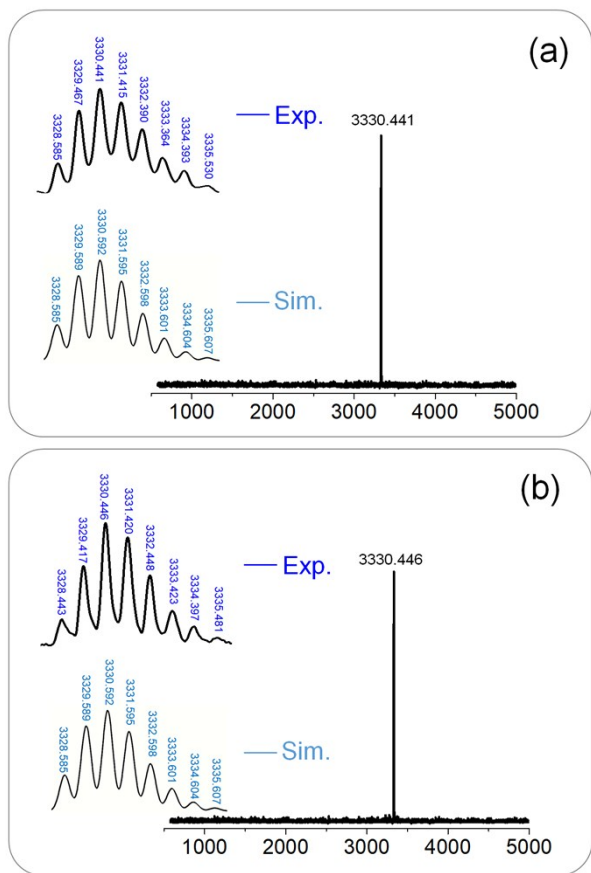


Fig. S1 MALDI-TOF mass spectra of **R-1** (a) and **S-1** (b) with both experimental and simulated isotopic mass spectroscopic patterns.

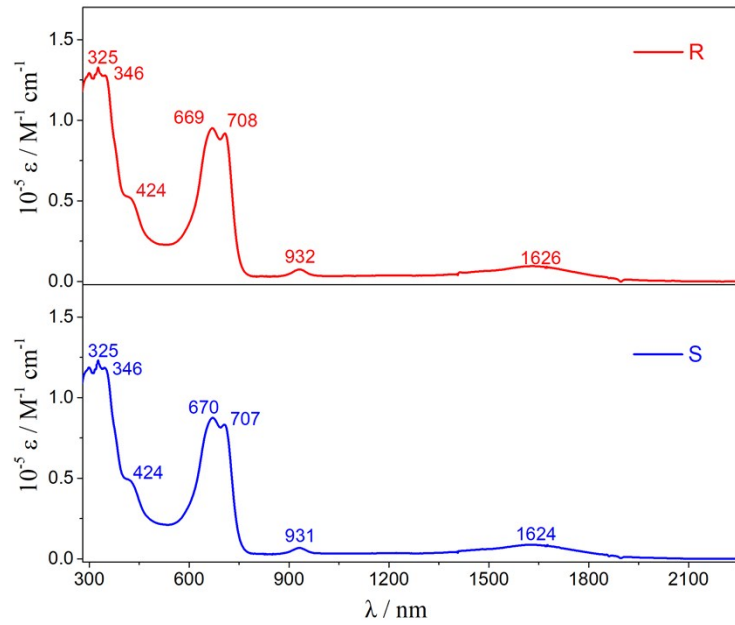


Fig. S2 Electronic absorption of (R)/(S)-[Pc(OBNP)₄]Tb{Pc[N(C₄H₉)₂]₈} (**R/S-1**) in CHCl₃.

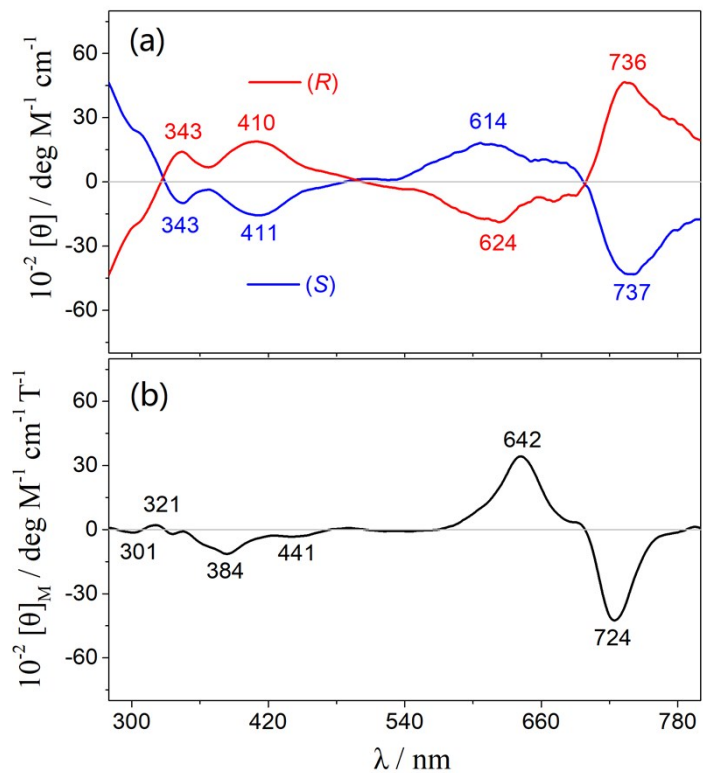


Fig. S3 (a) ORD spectra of $(R)/(S)$ - $[\text{Pc(OBNP)}_4]\text{Tb}\{\text{Pc}[\text{N}(\text{C}_4\text{H}_9)_2]_8\}$ (**R/S-1**) in CHCl_3 . Red and blue lines are used to plot the ORD spectra of the (R) - and (S) -enantiomer, respectively. (b) MCD spectrum of **S-1** in CHCl_3 .

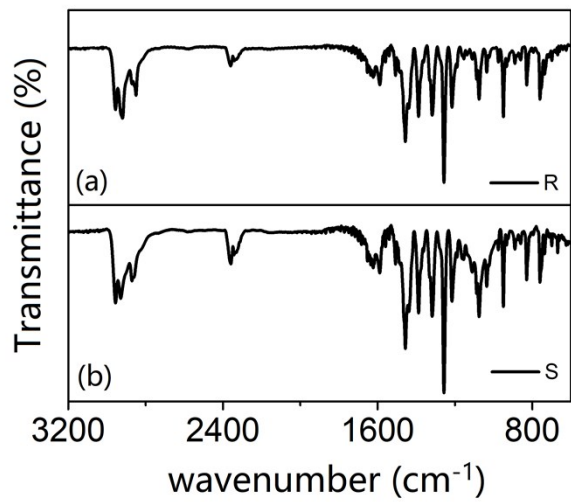


Fig. S4 IR spectra of $(R)/(S)$ - $[\text{Pc}(\text{OBNP})_4]\text{Tb}\{\text{Pc}[\text{N}(\text{C}_4\text{H}_9)_2]_8\}$ (**R/S-1**).

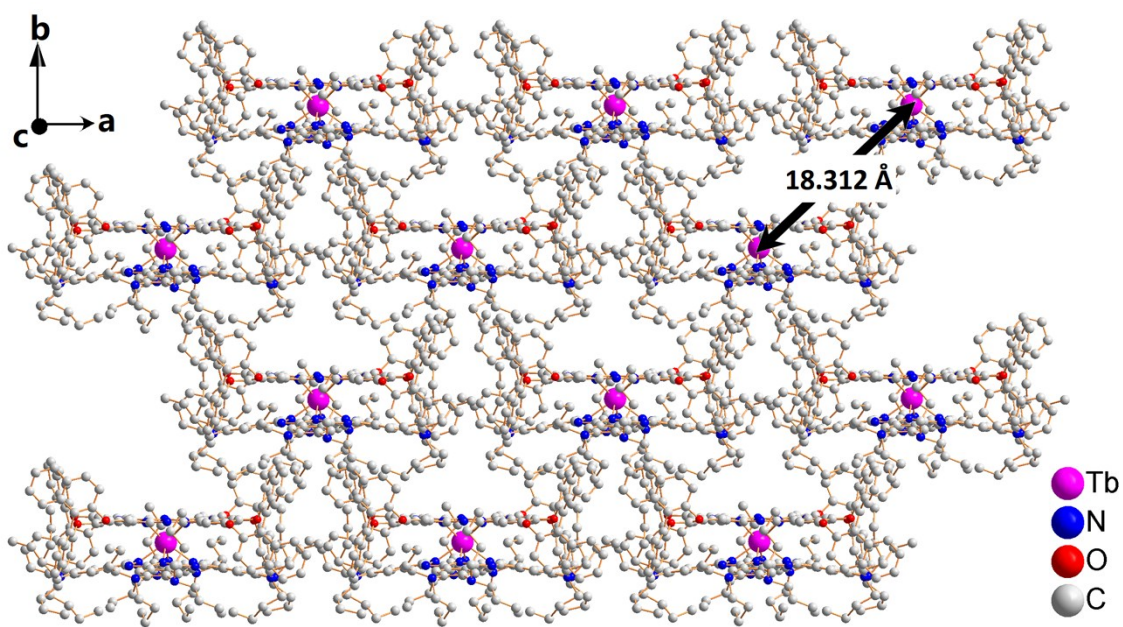


Fig. S5. Molecular packing in single crystals of *R*-1 with all H atoms omitted for clarity.

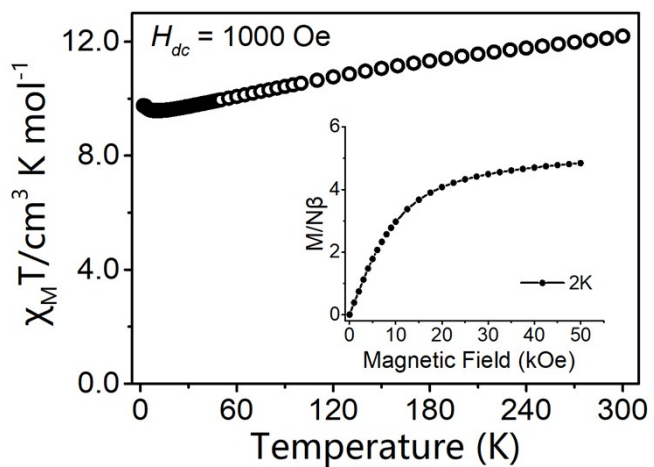


Fig. S6 Temperature dependence of $\chi_M T$ for **R-1** by experimental measurement with the M vs H curve at 2.0 K.

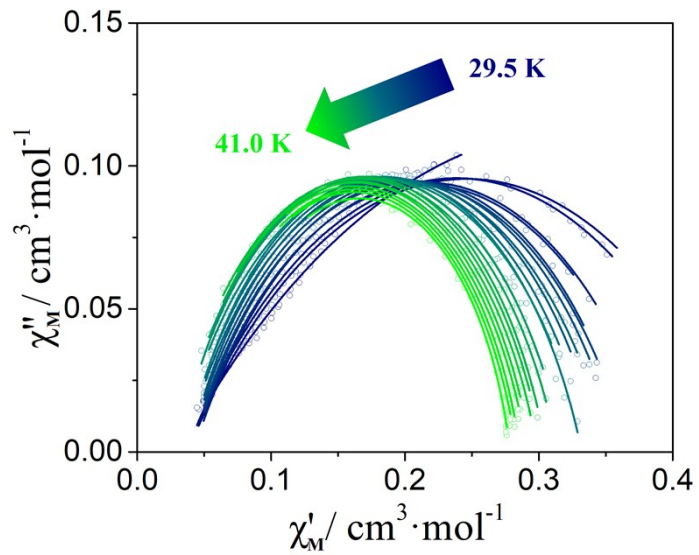


Fig. S7 Cole-Cole diagrams of **R-1** with the ac susceptibility data at 29.5-41.0 K under a zero applied dc field. The solid lines are the best fit to Debye's law.

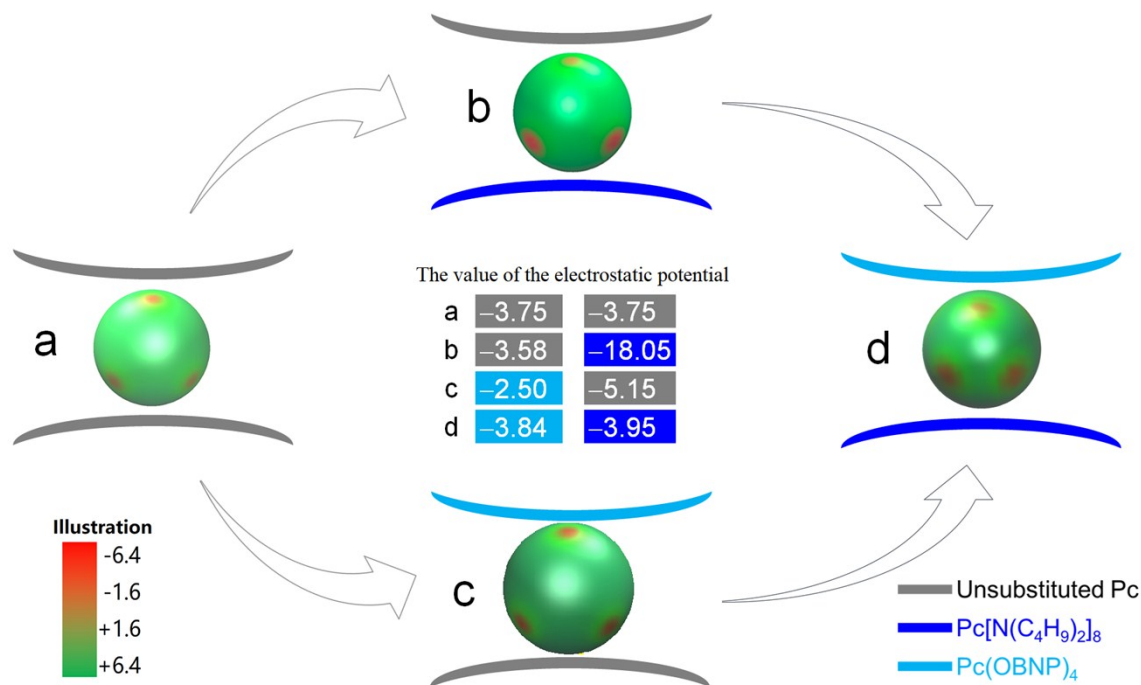


Fig. S8 Electrostatic potential projection on a 2.015 Å radius sphere centered in the Tb(III) position caused by the two phthalocyanine ligands in Tb(Pc)₂ (a), (Pc)Tb{Pc[N(C₄H₉)₂]₈} (b), (S)-(Pc)Tb[Pc(OBNP)₄] (c), and (R)-[Pc(OBNP)₄]Tb{Pc[N(C₄H₉)₂]₈} (**R-1**) (d).

Table S1. Analytical and mass spectrometric data for (*R*)/(*S*)-[Pc(OBNP)₄]Tb{Pc[N(C₄H₉)₂]₈} (***R/S-1***).^a

Compound	[M+H] ⁺ (m/z)	Analysis		
		C	H	N
<i>R-1</i>	3330.441 (3330.592) ^b	75.04 (75.00)	6.14 (6.29)	9.93 (10.09)
<i>S-1</i>	3330.446 (3330.592) ^b	74.88 (75.00)	6.20 (6.29)	10.09 (10.09)
[a]	Calculated values given in parentheses.	[b]	By MALDI-TOF mass spectrometry.	

Table S2. Electronic absorption data for (*R*)/(*S*)-[Pc(OBNP)₄]Tb{Pc[N(C₄H₉)₂]₈} (***R/S-1***) in CHCl₃.

Compound	$\lambda_{\text{max}}/\text{nm} (\log \varepsilon)$						
<i>R-1</i>	325 (5.13)	346 (5.10)	424 (4.71)	669 (4.98)	708 (4.96)	932 (3.88)	1626 (3.98)
<i>S-1</i>	325 (5.10)	346 (5.08)	424 (4.69)	670 (4.94)	707 (4.92)	931 (3.93)	1624 (3.94)

Table S3. CD spectrum data of (*R*)-[Pc(OBNP)₄]Tb{Pc[N(C₄H₉)₂]₈} (**R-1**) in CHCl₃.

λ (nm)	$10^{-3} [\theta]$ (deg·M ⁻¹ ·cm ⁻¹)	$10^{-3} g$
716	4.57	1.62
643	2.46	0.943
381	2.52	0.961
326	4.91	1.10

Table S4. Crystal data and structure refinements for **R-1**.^a

Compound	R-1
formula	C ₂₀₈ H ₂₀₈ N ₂₄ O ₈ Tb
fw	3330.90
crystal system	Monoclinic
space group	<i>C</i> 2
<i>a</i>	30.0327(18)
<i>b</i>	20.961(3)
<i>c</i>	21.2363(13)
α	90.00
β	135.00
γ	90.00
<i>V</i>	9452.8(17)
<i>Z</i>	2
θ range (deg)	2.94-54.95
<i>F</i> _{calcd} (g/cm ³)	1.170
μ (mm ⁻¹)	2.330
<i>F</i> (000)	3506
R ₁ (<i>I</i> >2 <i>θ</i>)	0.1484
R _{w2} (<i>I</i> >2 <i>θ</i>)	0.3524
R _{w2} for all	0.3816
<i>GOF</i> on F ²	1.282
CCDC number	1845654

[a] In this structure, the unit cell includes a large region of disordered solvent molecules, which could not be modeled as discrete atomic sites. We employed PLATON/SQUEEZE to calculate the diffraction contribution of the solvent molecules and, thereby, to produce a set of solvent-free diffraction intensities. The SQUEEZE calculations showed a total solvent accessible area volume of 1588 Å³ and the residual electron density amounted to 380 electrons per unit cell, corresponding to nearly 4 chloroform molecules and 8 methanol molecules (about 2 chloroform and 4 methanol molecule per asymmetric unit).

Table S5. Structural data for (*R*)-[Pc(OBNP)₄]Tb{Pc[N(C₄H₉)₂]₈} (**R-1**).

Compound	R-1
Average Tb–N [Pc(OBNP) ₄] bond distance [Å]	2.445
Average Tb–N {Pc[N(C ₄ H ₉) ₂] ₈ } bond distance [Å]	2.400
Tb–N ₄ [Pc(OBNP) ₄] plane distance [Å]	1.428
Tb–N ₄ {Pc[N(C ₄ H ₉) ₂] ₈ } plane distance [Å]	1.396
Interplanar distance [Å]	2.824
Dihedral angle between the two N ₄ planes [°]	0.00
Average twist angle [°]	38.84
The nearest Tb...Tb distance [Å]	18.312

Table S6. Relaxation fitting parameters for **R-1** from Least-Squares Fitting data of $\chi(f)$ between 1- 999 Hz under zero dc field.

T / K	χ_T	χ_S	τ / s	α
29.5	0.537	0.0312	3.51E-02	0.485
30.0	0.454	0.0376	3.01E-02	0.453
30.5	0.441	0.0365	2.52E-02	0.437
31.0	0.391	0.0419	1.94E-02	0.370
31.5	0.390	0.0396	1.67E-02	0.377
32.0	0.369	0.0412	1.27E-02	0.332
32.5	0.367	0.0393	1.03E-02	0.338
33.0	0.361	0.0383	8.29E-03	0.323
33.5	0.347	0.0384	6.45E-03	0.294
34.0	0.353	0.0349	5.37E-03	0.315
34.5	0.340	0.0347	4.01E-03	0.290
35.0	0.332	0.0362	3.22E-03	0.266
35.5	0.335	0.0302	2.50E-03	0.288
36.0	0.319	0.0308	1.92E-03	0.250
36.5	0.319	0.0289	1.53E-03	0.255
37.0	0.314	0.0282	1.18E-03	0.251
37.5	0.306	0.0315	9.28E-04	0.221
38.0	0.303	0.0283	7.53E-04	0.226
38.5	0.299	0.0300	5.95E-04	0.221
39.0	0.294	0.0319	4.82E-04	0.207
39.5	0.291	0.0331	3.89E-04	0.206
40.0	0.286	0.0399	3.32E-04	0.184
40.5	0.283	0.0408	2.65E-04	0.182
41.0	0.279	0.0535	2.38E-04	0.150

Table S7. The electrostatic potential values caused by the two phthalocyanine ligands with the magnetic properties.

Compounds	Electrostatic potential values / a.u.			Magnetic properties		Ref.
	Pc	Pc[N(C ₄ H ₉) ₂]	Pc(OBNP) ₄	<i>U</i> _{eff} /K	<i>T</i> _B ^a /K	
Tb(Pc) ₂	-3.75	—	—	590	—	S5
(Pc)Tb{Pc[N(C ₄ H ₉) ₂] ₈ }	-3.58	-18.05	—	939	30	S6
(S)-(Pc)Tb[Pc(OBNP) ₄]	-5.15	—	-2.50	847	28	S7
(R)-[Pc(OBNP) ₄]Tb{Pc[N(C ₄ H ₉) ₂] ₈ }	—	-3.95	-3.84	638	25	This work

[a] Here, the magnetic blocking temperature (*T*_B) is the highest temperature at which an SMM displays hysteresis in plots of magnetization (M) *versus* magnetic field (H). It is worth noting that the value of *T*_B strongly depends on the sweep rate of the field.

References for ESI

- [S1] (a) K. S. Cole and R. H. Cole, *J. Chem. Phys.*, 1941, 9, 341-351; (b) K. S. Cole and R. H. Cole, *J. Chem. Phys.*, 1942, 10, 98-105; (c) S. M. J. Aubin, Z. Sun, L. Pardi, J. Krzystek, K. Folting, L.-C. Brunel, A. L. Rheingold, G. Christou and D. N. Hendrickson, *Inorg. Chem.*, 1999, 38, 5329-5340.
- [S2] M. J. Frisch, G. W. Trucks, H. B. Schlegel, G. E. Scuseria, M. A. Robb, J. R. Cheeseman, G. Scalmani, V. Barone, B. Mennucci, G. A. Petersson, H. Nakatsuji, M. Caricato, X. Li, H. P. Hratchian, A. F. Izmaylov, J. Bloino, G. Zheng, J. L. Sonnenberg, M. Hada, M. Ehara, K. Toyota, R. Fukuda, J. Hasegawa, M. Ishida, T. Nakajima, Y. Honda, O. Kitao, H. Nakai, T. Vreven, J. A. Montgomery, Jr., J. E. Peralta, F. Ogliaro, M. Bearpark, J. J. Heyd, E. Brothers, K. N. Kudin, V. N. Staroverov, T. Keith, R. Kobayashi, J. Normand, K. Raghavachari, A. Rendell, J. C. Burant, S. S. Iyengar, J. Tomasi, M. Cossi, N. Rega, J. M. Millam, M. Klene, J. E. Knox, J. B. Cross, V. Bakken, C. Adamo, J. Jaramillo, R. Gomperts, R. E. Stratmann, O. Yazyev, A. J. Austin, R. Cammi, C. Pomelli, J. W. Ochterski, R. L. Martin, K. Morokuma, V. G. Zakrzewski, G. A. Voth, P. Salvador, J. J. Dannenberg, S. Dapprich, A. D. Daniels, O. Farkas, J. B. Foresman, J. V. Ortiz, J. Cioslowski, and D. J. Fox, *Gaussian 09, Version D.01*, Gaussian, Inc., Wallingford CT, 2013.
- [S3] T. Lu and F. Chen, *J. Comput. Chem.*, 2012, 33, 580-592.
- [S4] W. Humphrey, A. Dalke and K. Schulten, *J. Mol. Graphics*, 1996, 14, 33-38.
- [S5] N. Ishikawa, M. Sugita, N. Tanaka, T. Ishikawa, S.-Y. Koshihara and Y. Kaizu, *Inorg. Chem.*, 2004, **43**, 5498-5500.
- [S6] Y. Chen, F. Ma, X. Chen, B. Dong, K. Wang, S. Jiang, C. Wang, X. Chen, D. Qi, H. Sun, B. Wang, S. Gao and J. Jiang, *Inorg. Chem.*, 2017, **56**, 13889-13896.
- [S7] K. Wang, F. Ma, D. Qi, X. Chen, Y. Chen, Y.-C. Chen, H.-L. Sun, M.-L. Tong and J. Jiang, *Inorg. Chem. Front.*, 2018, **5**, 939-943.